Cholesterol Distribution in Living Cells: Fluorescence Imaging Using Dehydroergosterol as a Fluorescent Cholesterol Analog

Sushmita Mukherjee,* Xiaohui Zha,* Ira Tabas,# and Frederick R. Maxfield*

*Department of Biochemistry, Cornell University Medical College, New York, New York 10021, and #Departments of Medicine and Anatomy and Cell Biology, College of Physicians and Surgeons, Columbia University, New York, New York 10032 USA

ABSTRACT Cholesterol is an important constituent of most mammalian cell membranes and its concentration in various cellular membranes is tightly regulated. Although there is much information about cholesterol distribution and trafficking in cells, it is primarily derived from indirect measurements, and the results obtained using different approaches are often conflicting. A cholesterol analog that faithfully mimics the properties of cholesterol and can be followed in living cells would thus be very useful. In this study, we report the fluorescence imaging of such an analog, dehydroergosterol (DHE), in living cells. DHE differs from cholesterol in having three additional double bonds and an extra methyl group. In model systems, DHE closely mimics the behavior of native cholesterol. Using triple-labeling studies, we show that DHE colocalizes extensively with endocytosed transferrin, an endocytic recycling compartment marker, and with a marker for the *trans*-Golgi network, Tac-TGN38. This distribution of DHE is qualitatively similar to that observed when cells are labeled with the fluorescent cholesterol-binding polyene antibiotic, filipin, although there are differences in apparent proportions of DHE and filipin that are localized at the plasma membrane. Another cholesterol derivative, 25-NBD-cholesterol, has a structure that is compromised by the presence of a bulky NBD group and does not distribute to the same organelles as DHE or filipin. In addition, we show in this manuscript that kinetic processes can be followed in living cells by monitoring recovery of DHE fluorescence in a photobleached region over time. Our observations provide evidence for the presence of a large intracellular cholesterol pool in the endocytic recycling compartment and the *trans*-Golgi network that might play important roles in the trafficking of lipids, lipid-anchored proteins, and transmembrane proteins that preferentially partition into cholesterol-enriched membrane domains. In addition, this intracellular cholesterol pool might be involved in the maintenance of cellular cholesterol homeostasis.

INTRODUCTION

Most mammalian cells contain cholesterol as a component of their cellular membranes. Cholesterol levels in cells are stringently controlled, and while it is necessary for cell survival, excess cholesterol can lead to cytotoxic effects (Tabas, 1997). In model membrane systems cholesterol organization within a bilayer as well as its effects on host bilayer properties have been found to be a complex function of the host membrane composition and the precise amount of cholesterol present (Almeida et al., 1993; Vaz and Almeida, 1993; Harris et al., 1995; Mukherjee and Chattopadhyay, 1996; Silvius et al., 1996; Ahmed et al., 1997). This, in addition to the fact that cholesterol preferentially interacts with a subset of membrane lipids and proteins (Yeagle, 1985; Schroeder et al., 1995), has given rise to the idea of specialized microdomains (or "rafts") that might play important roles in several cellular functions such as signaling, adhesion, and motility (Simons and Ikonen, 1997). Indeed, structurally and kinetically distinct cholesterol-rich and -poor domains have been detected in cellular membranes (Schroeder et al., 1991).

In addition to such functionally important regionalization within a bilayer, cholesterol has been reported to be distributed heterogeneously among various intracellular membranes. By several estimates, as high as 80–90% of total cellular cholesterol is present at the plasma membrane at steady state (Lange, 1991). On the contrary, the endoplasmic reticulum and mitochondrial inner membranes contain very little cholesterol (Severs, 1982; Lange, 1991). This observation, a priori, is difficult to reconcile with the rapid flip-flop and spontaneous intermembrane transfer rates observed for cholesterol in model membranes (Yeagle, 1985; Schroeder et al., 1995), which should act to scramble and randomize cholesterol composition of all cellular membranes. Thus, in order to understand the functional roles of cholesterol in mammalian cells, it is important to under-

Received for publication 23 March 1998 and in final form 16 July 1998.

Address reprint requests to Frederick R. Maxfield, Department of Biochemistry, Cornell University Medical College, 1300 York Avenue, New York, NY 10021. Tel.: 212-746-6405; Fax: 212-746-8875; E-mail: frmaxfie@mail.med.cornell.edu.

S. Mukherjee and X. Zha contributed equally to this study.

This paper is dedicated to the memory of Dr. Fred Fay (University of Massachusetts), who was a pioneer in the application of digital imaging microscopy to solve problems in cell biology and physiology. His insightful advocacy of the use of cooled CCD cameras and his efforts to optimize detectors for biological applications contributed significantly to the technology that made this study possible.

Abbreviations used: DHE, dehydroergosterol ($\Delta^{5,7,9(11)22}$-ergostatetraen-3β-ol); ACAT, acyl CoA:cholesterol acyltransferase; CHO, Chinese hamster ovary; DIC, differential interference contrast; DMSO, dimethylsulfoxide; DOPC, dioleoylphosphatidylcholine; ERC, endocytic recycling compartment; FITC, fluorescein isothiocyanate; HMG-CoA reductase, hydroxymethylglutaryl CoA reductase; HPLC, high performance liquid chromatography; MitoTracker Red, chloromethyl X-rosamine; 22-NBD-cholesterol, 22-(*N*-(7-nitrobenz-2-oxa-1,3-diazol-4-yl)amino)-23,24-bisnor-5-cholen-3β-ol; 25-NBD-cholesterol, 25-[*N*-[(7-nitrobenz-2-oxa-1,3-diazol-4-yl)-methyl]amino]-27-norcholesterol; PBS, phosphate buffered saline; Tf, transferrin; TGN, *trans*-Golgi network; UV, ultraviolet.

0006-3495/98/10/1915/11 $2.00

stand cholesterol trafficking mechanisms vis-à-vis the principles governing its distribution and retention within and among membranes.

Several methods are available to study cholesterol distribution and trafficking in cells (reviewed in Liscum and Dahl, 1992; Liscum and Underwood, 1995). However, all these methods are rather indirect, and although they provide significant information about cellular cholesterol distribution and trafficking, often suffer from serious limitations (Liscum and Dahl, 1992; Liscum and Underwood, 1995). Thus, a reliable analog of cholesterol that can be easily followed in a living cell would provide a very useful experimental tool to address questions regarding cholesterol distribution in unperturbed cells. Fluorescent cholesterol analogs offer such a possibility, since they can be followed by fluorescence microscopy, which has the advantage of being able to study a relatively large population of cells, while providing quantitative information about the spatial distribution of a fluorescent molecule that can be followed in real time.

Obtaining a cholesterol analog that faithfully mimics cholesterol is not simple. Cholesterol is composed of an approximately planar steroid ring system, with a 3β-hydroxyl function on one end and a hydrophobic alkyl tail on the other (Yeagle, 1985; Schroeder et al., 1995) (see Fig. 1 *a*). The hydroxyl group anchors the molecule at the membrane interface, so that cholesterol inserts into a membrane leaflet approximately parallel to the fatty acyl chains of the surrounding lipids (Yeagle, 1985; Schroeder et al., 1995). Several studies have shown that in order to obtain a biologically active cholesterol analog, it is necessary for the derivative to have an intact alicyclic chain, a free 3β-OH, a planar $\Delta^{5(6)}$ double bond, angular methyl groups, and a branched seven-carbon alkyl chain at the 17β-position (Duax et al., 1988; Schroeder et al., 1991, 1995). This severely limits the chemical modifications that can be imposed on cholesterol structure without compromising the ability of the derivative to faithfully mimic cholesterol.

DHE is a fluorescent cholesterol analog that satisfies all the above criteria, differing from cholesterol only in having three additional double bonds and an extra methyl group (Schroeder et al., 1991) (Fig. 1 *b*). Two of the additional double bonds are in the steroid ring system, and along with the $\Delta^{5(6)}$ double bond of cholesterol form a conjugated double bond system that presumably makes the molecule fluorescent. When bound to DOPC liposomes (see Fig. 2), DHE exhibits structured absorption and emission spectra, with the absorption peaks around 310, 324, and 338 nm and emission peaks around 354, 375, 394, and 414 nm. This cholesterol analog is unlike most synthetic analogs that contain a bulky reporter group that either cuts short the seven-member alkyl chain (Fig. 1 *c*, 25-NBD-cholesterol), or replaces the 3β-OH group (example not shown). DHE is a natural product, comprising up to 20% of some yeast membrane sterols (Schroeder et al., 1991). Various studies in model membrane systems as well as isolated organellar membranes have shown that DHE closely mimics the behavior of radiolabeled cholesterol (Schroeder et al., 1991, 1995), and a replacement of up to 85% of the endogenous sterol of some cultured fibroblasts with DHE has no significant effect on growth properties, membrane composition, or activities of membrane enzymes (Schroeder et al., 1991, 1995). In addition, erg9 mutants of yeast, which are auxotrophs for ergosterol in their aerobic growth, can grow in media supplemented with DHE as the sole sterol source (A. H. Tinkelenberg and S. L. Sturley, College of Physicians and Surgeons, Columbia University, New York, NY; personal communication).

Despite of the characterization of DHE and its use in fluorescence spectroscopic studies, there have been, to our knowledge, no reports on the microscopic imaging of this cholesterol analog. The difficulty in imaging DHE comes from the fact that it absorbs in the UV region of the spectrum and emits in the UV and blue regions (see Fig. 2). The sensitivities of most detectors for fluorescence micros-

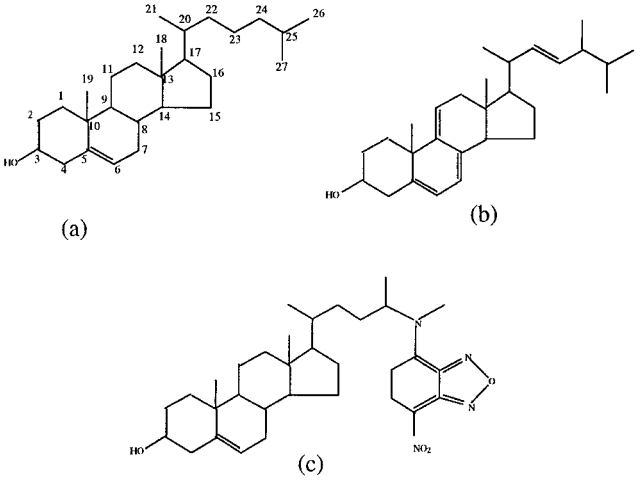

FIGURE 1 Chemical structures of (*a*) cholesterol, (*b*) dehydroergosterol (DHE), and (*c*) 25-NBD-cholesterol. The numbers in (*a*) represent the conventional nomenclature of the carbon atoms in cholesterol.

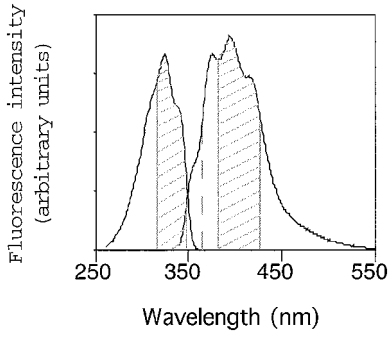

FIGURE 2 Excitation and emission spectra of 1 mol % DHE in DOPC multilamellar vesicles. Excitation and emission bandpass of 7 nm were used for all experiments. The hatched bars in the spectra represent the bandpasses of the excitation and emission filters used in this study for UV imaging. The dotted line represents the wavelength selection by the dichromatic mirror.

copy fall off sharply in the UV region. Furthermore, many optical components of the microscope, unless specifically designed for UV transmission, absorb strongly in this wavelength range (Dunn and Maxfield, 1998). In this manuscript we report the imaging of DHE fluorescence in live cells labeled to steady state using a specially designed camera with a back-thinned cooled charge coupled device (CCD) chip that has a quantum efficiency of ~70% at 400 nm. The high quantum efficiency and low noise of cooled CCD cameras (Moore et al., 1990) as well as the high UV throughput of various optical components of the microscope were essential for these studies.

MATERIALS AND METHODS

Materials

The fluorescent cholesterol analog, DHE, and the cholesterol-binding antibiotic, filipin, were obtained from Sigma Chemical Co. (St. Louis, MO). Purity of DHE was confirmed by HPLC following a previously published protocol (Fischer et al., 1984). Cy-3 was obtained as a protein conjugation kit from Amersham Life Sciences (Pittsburgh, PA). Human Tf was obtained from Sigma Chemical Co. It was then iron-loaded and further purified by Sephacryl S-300 gel filtration as described previously (Yamashiro et al., 1984). Cy-3 was conjugated to the iron-loaded Tf following manufacturer's instructions. Labeled Tf was dialyzed thoroughly to remove unbound Cy-3. FITC, 22-NBD-cholesterol, and MitoTracker Red (chloromethyl X-rosamine) were obtained from Molecular Probes, Inc. (Eugene, OR). 25-NBD-cholesterol was a kind gift from Dr. A. Chattopadhyay and was originally acquired from Molecular Probes, Inc. FITC-labeled anti-Tac antibody was prepared as described (Humphrey et al., 1993; Johnson et al., 1996). DOPC was obtained from Avanti Polar Lipids (Birmingham, AL). All tissue culture supplies were from GIBCO-BRL (Gaithersburg, MD). All other chemicals were from Sigma Chemical Co.

Preparation of liposomes and spectroscopic measurements

DHE-containing multilamellar vesicles were prepared as follows. DOPC (320 nmol) and 3.2, 1.6, and 0.32 nmol of DHE were added in separate test tubes from ethanolic stock solutions. Control liposomes were prepared with DOPC only. A few drops of chloroform was added to each tube and vortexed to mix. The lipids were then dried under argon to form a thin film and subsequently incubated overnight under vacuum. After the lipid films had dried thoroughly, 1.5 ml PBS (pH 7.4) was added to each test tube, followed by vortexing for 3 min. Fluorescence excitation spectra were recorded by setting the emission wavelength at 376 nm, while for obtaining emission spectra, the excitation wavelength was set at 324 nm. Background spectra obtained from liposomes containing DOPC only were subtracted from all DHE spectra. Both excitation and emission bandpasses were set at 7 nm for all experiments. All spectra were acquired using a Spex Fluorolog spectrofluorometer (Spex Industries, Inc., Edison, NJ). The spectra obtained matched very well with those previously reported (Schroeder et al., 1987), except that we obtained an additional peak in the emission spectrum (414 nm). We have shown in Fig. 2 the spectrum obtained in DOPC liposomes containing 1 mol % DHE. We obtained identical spectra for liposomes containing 0.1 and 0.5 mol % DHE with roughly linear increase in the integrated intensity.

Cells and cell culture

TRVb-1/Tac-TGN38 cells used in this study are a CHO cell line expressing both the human Tf receptor and a Tac-TGN38 construct containing the extracellular domain of the interleukin-2 receptor α-chain (T cell antigen or Tac) with the cytoplasmic and transmembrane domains of TGN38 (Humphrey et al., 1993; Johnson et al., 1996). The cells were grown in bicarbonate-buffered Hams F-12 medium supplemented with 5% fetal bovine serum (FBS), 100 U/ml penicillin, 100 μg/ml streptomycin, 400 μg/ml geneticin, and 400 U/ml hygromycin. Geneticin and hygromycin were used as selection markers for the transfected transferrin receptors and the Tac-TGN38 construct, respectively. All cells were grown in a 5% CO_2 environment in humidified incubators at 37°C.

Fluorescence labeling of cells

A stock solution (5 mM) of DHE was made in ethanol and stored at −86°C under argon. To label cells with DHE, semi-confluent cell monolayers were grown for 16–20 h in bicarbonate buffered Hams F-12 medium supplemented with 5% lipoprotein depleted serum (LPDS) containing 12.5 μM DHE added from an ethanolic stock solution (final ethanol concentration 0.25% v/v). LPDS was used instead of complete serum because it does not contain lipoproteins that could back exchange DHE from the plasma membrane. After the incubation, cell monolayers were washed two times with PBS. Microscopy at this stage, however, showed that although the cells were efficiently labeled with DHE, there were many particles of DHE in the background and occasionally on the cells, making it difficult to distinguish truly incorporated label from exogenous label. This particulate DHE could not be removed even by subjecting the cells to treatments akin to the back exchange protocol that can efficiently remove short chain lipid analogs that are already incorporated in the outer leaflet of the plasma membrane (Koval and Pagano, 1989; Mayor et al., 1993). Thus, trypsinization and thorough washing of the cells followed by replating was used to separate labeled cells from the DHE particles. The labeled cells were trypsinized for 5 min at 37°C, washed twice more with PBS by centrifugation at ~135 × *g* in a table top centrifuge (Sorvall T6000D; Sorvall, Inc., Newtown, CT) and resuspension, and finally resuspended in Hams F-12 medium containing 5% LPDS. The cells were then plated for microscopy on 35-mm plastic tissue culture dishes whose bottoms were replaced with poly-D-lysine-coated coverslips as described previously (Salzman and Maxfield, 1989). After replating, cells were allowed to grow for an additional 16–20 h to allow complete recovery from trypsinization and to attain a well-spread morphology before further experimental manipulations. For the localized photobleaching experiments reported here, cells were grown on coverslips coated with 100 μg/ml fibronectin (instead of poly-D-lysine) so that the cells were flatter and better spread out. However, additional experiments using cells grown on poly-D-lysine-coated coverslips showed essentially identical behavior.

Intracellular distribution of DHE was compared to that of the Tac-TGN38 construct labeled with fluorescein-conjugated anti-Tac antibody and Cy-3-labeled transferrin. Cells labeled to steady state with DHE were washed several times with isotonic medium 1 (150 mM NaCl, 5 mM KCl, 1 mM $CaCl_2$, 1 mM $MgCl_2$, and 20 mM HEPES, pH 7.4; supplemented with 2 g/l glucose), and incubated in this medium at 37°C on a table top slide warmer. A labeling solution containing a mixture of 1 μg/ml each of FITC-anti-Tac antibody and Cy3-Tf in medium 1 was centrifuged at 100,000 × *g* for 20 min in a Sorvall RC M120EX ultracentrifuge (Sorvall, Inc.) and the supernatant warmed to 37°C. Cells were then incubated with this mixture for 10 min at 37°C, washed thoroughly, and then chased in medium 1 for 45 min. The live cells were then taken for imaging.

In separate experiments, cells were labeled with the fluorescent cholesterol binding drug, filipin, using a variation of a published method (Tabas et al., 1994). The cells were first rinsed with medium 1 several times and then fixed with 3% paraformaldehyde in PBS for 1 h at room temperature. The paraformaldehyde was rinsed with PBS and quenched with 50 mM glycine in PBS. Cells were then incubated for 2 h at room temperature in medium 1 containing 50 μg/ml filipin added from a stock solution in DMSO (final concentration 0.2% v/v). After the incubation, filipin was removed by rinsing the cells several times with medium 1. For experiments involving triple-labeling of cells with filipin, FITC-anti-Tac antibody, and Cy3-Tf, cells were first labeled with a mixture of the latter two fluorophores as described above, followed by fixation and labeling with filipin.

Fluorescence microscopy and quantitative image analysis

Fluorescence microscopy and digital image acquisition were carried out using a Leica DMIRB microscope (Leica Mikroscopie und Systeme GmbH, Germany) equipped with a Princeton Instruments (Princeton, NJ) cooled CCD camera driven by Image-1/MetaMorph Imaging System software (Universal Imaging Corporation, PA). All images were acquired using a high-magnification oil immersion objective (63× magnification, 1.4 numerical aperture). For the experiments presented here, it was essential to optimize the throughput of the microscope in the UV region of the spectrum. This was achieved, in part, by using a lamp housing from Leica with a collecting lens that had high transmittance characteristics in the UV region. DHE and filipin were imaged using a specially designed filter cube obtained from Chroma Technology Corp. (Brattleboro, VT) [335-nm (20-nm bandpass) excitation filter, 365-nm longpass dichromatic filter, and 405-nm (40-nm bandpass) emission filter; see Fig. 2]. The detection of UV fluorescence of DHE was made possible by the use of a camera with a back-thinned CCD chip (Princeton Instruments Frame Transfer Pentamax camera with a 512 × 512 back-thinned EEV chip; model 512EFTB). This camera has ~70% quantum efficiency at 400 nm. In the triple-label studies, FITC-anti-Tac and 25-NBD-cholesterol were imaged using a standard fluorescein filter cube [470-nm (20-nm bandpass) excitation filter, 510-nm longpass dichromatic filter, and 537-nm (23-nm bandpass) emission filter] and Cy3-Tf and MitoTracker Red using a standard rhodamine filter cube [535-nm (50-nm bandpass) excitation filter, 565-nm longpass dichromatic filter, and 610-nm (75-nm bandpass) emission filter]. Since the CCD camera used in this study has a fast readout rate (~15 frames/s for a 512 × 512 image), the focal plane in all cases was chosen by real-time focusing on a video monitor using DIC optics. This was especially important in DHE imaging since it photobleached readily when excited by UV light. In case of 25-NBD-cholesterol fluorescence, extensive cross-over of signal to the red (MitoTracker) channel was observed. The cross-over fraction was rather high for optimal mathematical correction. To overcome this constraint, we first acquired the NBD image, bleached it by keeping the shutter open for 1 min, and then acquired the MitoTracker Red and DHE images, in that order. In control experiments, we ensured that 1-min photobleaching with 470-nm excitation light bleached NBD fluorescence completely, with no effect on MitoTracker Red or DHE fluorescence.

For a quantitative estimate of the fraction of DHE or filipin fluorescence that is in the perinuclear region versus on the plasma membrane, the following methodology was used. The images were first corrected for background by subtracting a background value from the entire image. The background intensity was estimated from several intensity measurements in regions of the coverslip that did not contain any cells. The background intensity rarely exceeded 10% of the maximum pixel intensity, and was found to be quite uniform both within a coverslip as well as among several coverslips investigated on the same day. After background correction, a box (6 × 6 pixel dimension) was placed in the perinuclear fluorescent structure and three additional boxes of identical dimensions were placed on the plasma membrane. Average intensity in each box was determined, the values obtained from the three plasma membrane boxes were averaged, and a ratio of this averaged pixel intensity on the plasma membrane to that in the intracellular fluorescent compartment was determined. This measurement was repeated for ~20 cells from experiments done on two different days. This approach was also utilized to ensure photobleaching and fluorescence recovery by monitoring ratios in the bleached region and comparing it with those obtained from unbleached regions. Examples of such measurements are shown in Fig. 8. These measurements ensured that any changes in fluorescence intensity ratio after localized photobleaching or recovery was not simply because of a general photobleaching of the sample due to multiple image acquisitions.

For visual output purposes, the digital images were clipped to the relevant eight bits, transferred to a MacIntosh Power PC, intensity-mapped through logarithmic look-up tables (luts) using Adobe Photoshop, and printed on a dye sublimation printer (SpectraStar Dsx, General Parametrics Corporation, CA).

RESULTS

DHE and filipin labeling of CHO cells

Fig. 3 shows CHO cell line TRVb-1/TacTGN38 labeled with DHE (*a*) and filipin (*c*). Panels *b* and *d* show the autofluorescence levels of unlabeled cells imaged using identical acquisition and processing conditions as DHE and filipin, respectively. In both cases, signals clearly above autofluorescence levels are obtained. This is an important control inasmuch as cells can exhibit relatively high autofluorescence in this region of the spectrum. The overall staining pattern is quite similar with DHE and filipin, with significant fluorescence at the plasma membrane, as well as intracellular fluorescence in the perinuclear region. When the cells were imaged at a focal plane near the middle of the cells, a ring of fluorescence from the plasma membrane staining could often be seen. Furthermore, varying the concentration of DHE over a 10-fold concentration range provided very similar staining patterns with roughly linear increase in intensity. This observation ensures that we are operating below the self-quenching regime.

When the relative amounts of DHE on the cell surface and in the intracellular fluorescent spot were investigated quantitatively (see Materials and Methods for details), DHE appeared roughly two to threefold brighter in the intracellular spot than on the plasma membrane. The ratios of plasma membrane to intracellular intensities obtained with filipin staining varied much more from cell to cell. In general, the fraction of total filipin fluorescence that is localized at the plasma membrane was larger than the frac-

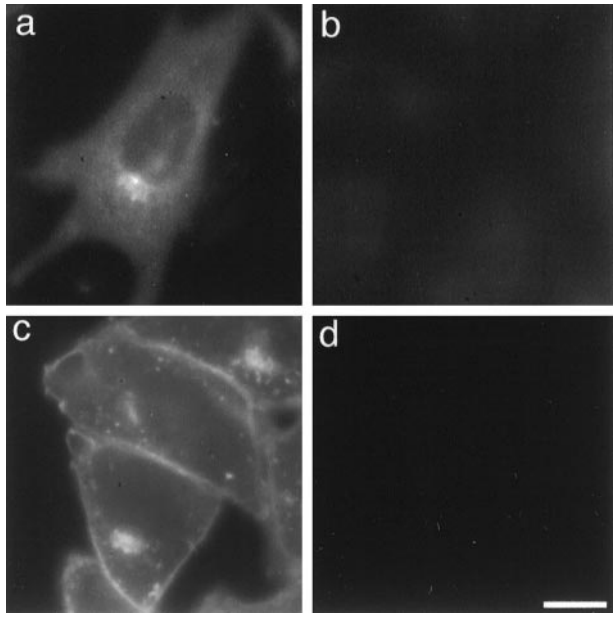

FIGURE 3 Labeling of the CHO cell line TRVb-1/TacTGN38 with 12.5 μM DHE (*a*) and 50 μg/ml filipin (*c*). See Materials and Methods for details of the labeling protocols. Panel *b* represents the autofluorescence from unlabeled cells under acquisition and processing conditions identical to DHE. Panel *d* represents a similar control for filipin fluorescence. Bar = 10 μm.

tion of DHE fluorescence at the plasma membrane. We discuss the possible reasons for a such a difference later. It should also be noted that while both DHE and filipin show qualitatively similar staining patterns, the cell surface morphology is compromised in case of cells labeled with filipin, and the cells appear to bleb extensively. The small bright spots on the cell surface in the filipin-labeled field often corresponded to folded-over or partly detached membrane fragments. This is an artifact of the fixation procedure, because similar blebbing is observed in unlabeled cells (detected by DIC) or DHE-labeled cells when they are also put through the same fixation protocol (data not shown).

25-NBD-cholesterol and DHE distributions differ significantly in CHO cells

Fig. 4 shows TRVb-1/TacTGN38 cells triple-labeled with DHE, 25-NBD-cholesterol, and MitoTracker Red. Briefly, cells were labeled for 16–20 h with a mixture of 12.5 μM DHE, 1.5 μM 25-NBD-cholesterol, and 5 nM MitoTracker Red in ethanol, with the final ethanol concentration not exceeding 0.3% v/v. After the incubation, the cells were washed, trypsinized, rewashed, and plated for microscopy as described in Materials and Methods. Upon microscopic investigation 16–20 h after replating, DHE was found to exhibit a staining pattern with most of the label either at the plasma membrane or in a perinuclear location (as shown in Fig. 3), while the NBD-cholesterol analog has a completely different steady-state distribution. Most of the structures labeled by 25-NBD-cholesterol appear to be mitochondria, as they colocalize extensively with MitoTracker Red, a mitochondrial marker (shown by small arrows in Fig. 4). In a minority (~2–5%) of the cells, some 25-NBD-cholesterol appears to colocalize with DHE in the intracellular fluorescent compartment (see Fig. 4, *a* and *b*; colocalization pointed out by large arrows). These regions are typically not labeled by MitoTracker Red. However, even in those cells that do show some colocalization of 25-NBD-cholesterol with DHE, most of the 25-NBD-cholesterol fluorescence is still localized at the mitochondria. The DHE fluorescence pattern, on the contrary, looks very similar to that of a steady-state distribution of C_6-NBD-sphingomyelin (Koval and Pagano, 1989; Mayor et al., 1993) or *FAST* DiI (S. Mukherjee, T. T. Soe, and F. R. Maxfield, submitted for publication), both of which are plasma membrane probes that are internalized and recycled efficiently (data not shown). Concentrations of up to 10 μM 25-NBD-cholesterol (roughly equimolar with DHE at the highest concentration) showed similar distribution as the one presented in Fig. 4, although the cells started blebbing significantly at the highest concentrations of 25-NBD-cholesterol. In addition, another NBD-cholesterol analog, 22-NBD-cholesterol, also showed distributions very similar to 25-NBD-cholesterol at steady state. In separate experiments, we found that incubations as short as 2 min with either 22- or 25-NBD-cholesterol resulted in distributions indistinguishable from those presented in Fig. 4. The mistargeting of NBD-cholesterol analogs is not unexpected because one of the requirements for a good cholesterol analog is an intact branched seven-carbon alkyl chain at the 17β-position (Duax et al., 1988; Schroeder et al., 1991, 1995). This is compromised, to varying degrees, in both the NBD-labeled cholesterol derivatives where the alkyl chain of cholesterol is cut short by the bulky and polar NBD group (Fig. 1 *c*). In fact, in either pure or mixed monolayers, 22-NBD-cholesterol has been shown not to mimic cholesterol, but to simply be excluded from regions of high packing densities in both cases (Slotte, 1995; Slotte and Mattjus, 1995). 25-NBD-cholesterol, however, has been previously shown to be a better mimic of cholesterol in model membrane systems (Mukherjee and

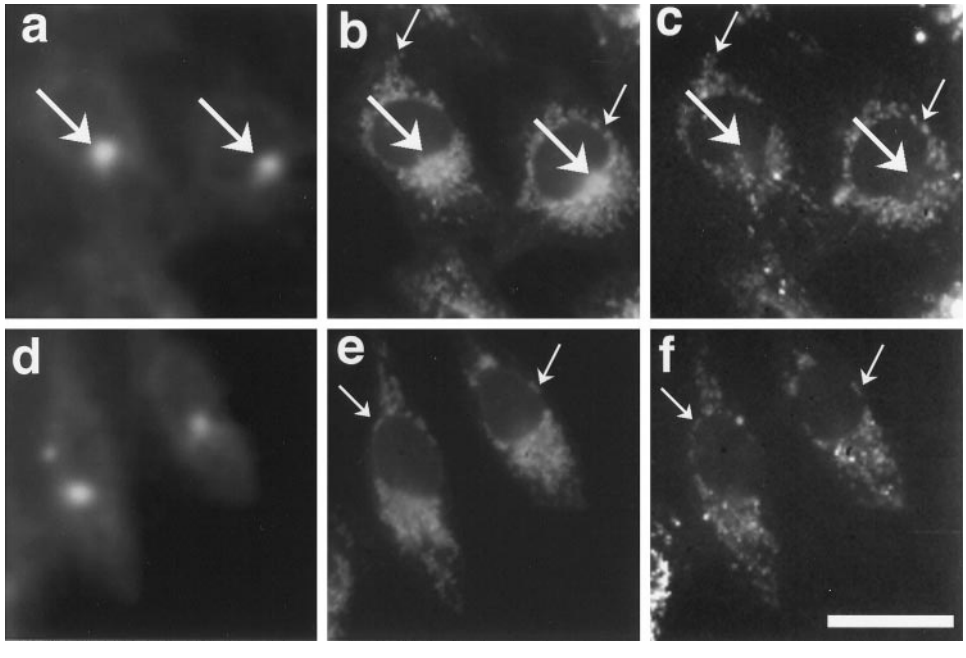

FIGURE 4 TRVb-1/TacTGN38 cells triple-labeled with 12.5 μM DHE (*a* and *d*), 1.5 μM 25-NBD-cholesterol (*b* and *e*), and 5 nM MitoTracker Red (*c* and *f*). Cells were labeled to steady state with all three probes. Panels *a–c* and *d–f* show two different fields of cells. See Materials and Methods for details. The small arrows (*b* and *c*) and (*e* and *f*) show regions of colocalization between 25-NBD-cholesterol and MitoTracker Red fluorescence. In a minority of cells, some of the 25-NBD-cholesterol fluorescence appears to colocalize with DHE in the intracellular fluorescent compartment that is devoid of the mitochondrial marker, while most of the 25-NBD-cholesterol is still localized in the mitochondria. The large arrows in *a–c* point out such colocalization of 25-NBD-cholesterol and DHE fluorescence. Bar = 10 μm.

Chattopadhyay, 1996); This does not appear to be the case when CHO cells are labeled to steady state with this probe.

DHE and filipin staining show high cholesterol concentrations in the plasma membrane, ERC, and TGN of CHO cells

Fig. 5 shows two sets of fields of TRVb-1/TacTGN38 cells, each labeled with three different probes: DHE (*a* and *d*; UV fluorescence), FITC-anti-Tac antibody (*b* and *e*; green fluorescence), and Cy3-Tf (*c* and *f*; red fluorescence). TacTGN38 has been shown to localize to the TGN in several different cell types, including the stably transfected line used in this study (Johnson et al., 1996). In the same cells, Cy3-Tf localizes predominantly to the ERC at steady state (Johnson et al., 1996). For the experiments presented here, cells were labeled with DHE as described in Materials and Methods. Under the experimental conditions used (10 min uptake of anti-Tac antibody and Tf, followed by a 45-min chase), most of the Tac-TGN38 bound to anti-Tac is in the TGN, while most of the Cy3-Tf is in the ERC (Johnson et al., 1996). Our results show that the intracellular DHE exhibits very good colocalization with endocytosed Tf (in the ERC). The TGN in CHO cells frequently surrounds the ERC (Johnson et al., 1996). As seen in Fig. 5, the DHE fluorescence in many of the cells covers an area larger than that covered by the Tf-labeled ERC. This DHE fluorescence surrounding the ERC colocalizes with the Tac-TGN38 distribution, suggesting that some DHE is also localized in the TGN in these cells.

Fig. 6 shows the TRVb-1/TacTGN38 cells labeled with filipin, FITC-anti-Tac antibody, and Cy3-Tf. Panels *a–c* and *d–f* show two different fields of cells, labeled with filipin (*a* and *d*), FITC-anti-Tac (*b* and *e*), and Cy3-Tf (*c* and *f*). The results appear quite similar to those obtained with DHE. In addition to an obvious presence of filipin in the ERC (as shown by colocalization with Cy3-Tf), there is also a clear colocalization of filipin and the anti-Tac antibody in the TGN (*arrows*).

Localized photobleaching of DHE fluorescence provides an approach for studying dynamic processes such as cholesterol trafficking in living cells

In Fig. 7 we present an experimental approach that can be used to investigate the kinetics of cholesterol trafficking in cells labeled to steady state with DHE. The cells were first labeled to steady state with DHE as described in Materials and Methods. The cell monolayer growing on coverslip dishes was rinsed several times with medium 1 warmed to 37°C. The dish was then placed on the microscope stage that was pre-set to 37°C and allowed to equilibrate. An area of cells was chosen by DIC and imaged (both DIC and DHE fluorescence). The field iris was then closed down so that only a fraction of the field was illuminated. This region was bleached by keeping the fluorescence shutter open for 1 min. The field iris was opened, and cells were imaged immediately after bleaching. The shutter was then closed, and the dish was kept on the microscope stage at 37°C for 20 min, and finally another DHE image of the field was acquired. We used 2 × 2 pixel binning while acquiring these images to reduce the acquisition time, so that multiple DHE fluorescence images could be acquired without substantial photobleaching. Results from two such experiments are shown in Fig. 7. Panels *a–c* and *d–f* show two different fields imaged for DHE fluorescence. Panels *a* and *d* show cells before photobleaching, panels *b* and *d* immediately

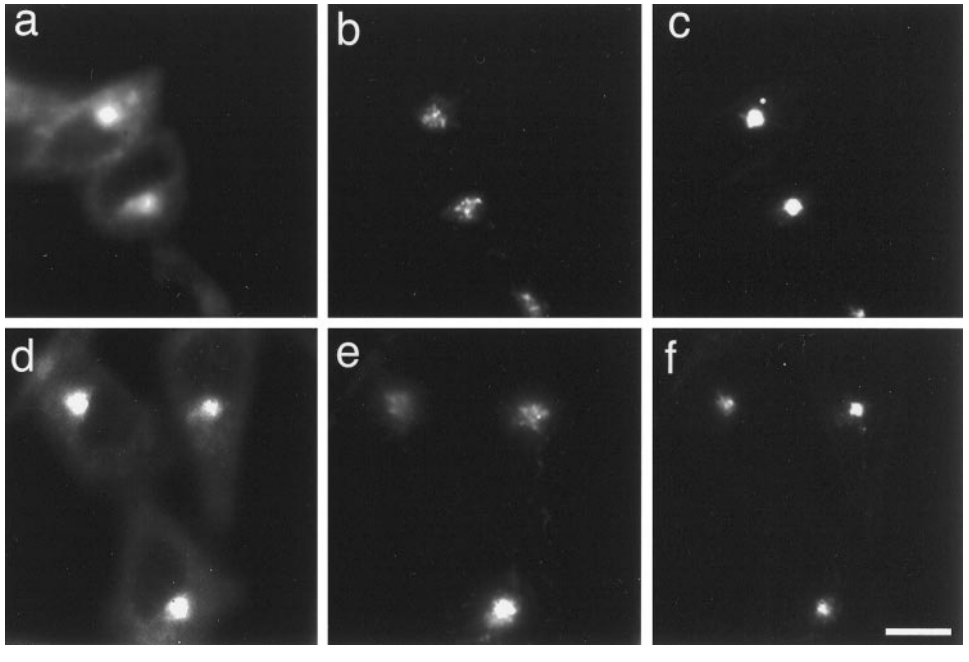

FIGURE 5 TRVb-1/TacTGN38 cells triple-labeled with 12.5 μM DHE (*a* and *d*), 1 μg/ml FITC-anti-Tac antibody (*b* and *e*), and 1 μg/ml Cy3-Tf (*c* and *f*). Cells were labeled to steady state with DHE as described in Materials and Methods, labeled for 10 min at 37°C with a mixture of 1 μg/ml each of FITC-anti-Tac antibody and Cy3-Tf, rinsed, and chased for 45 min in medium 1. Live cells were imaged immediately following the chase. Bar = 10 μm.

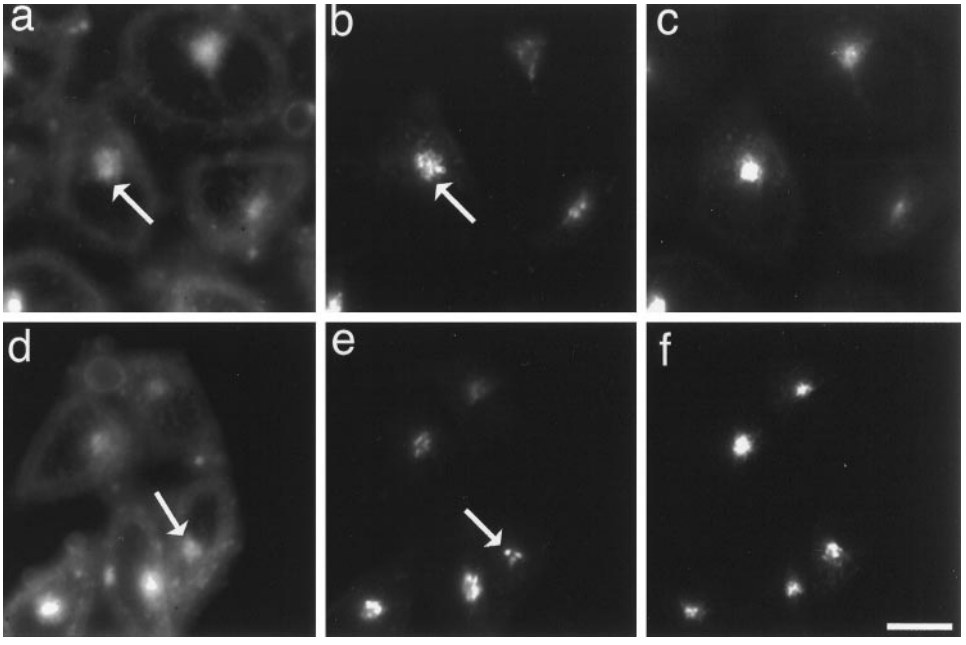

FIGURE 6 TRVb-1/TacTGN38 cells triple-labeled with 50 μg/ml filipin (*a* and *d*), 1 μg/ml FITC-anti-Tac antibody (*b* and *e*), and 1 μg/ml Cy3-Tf (*c* and *f*). Cells were first labeled with FITC-anti-Tac antibody and Cy3-Tf as described in the legend to Fig. 5. The cells were then fixed with paraformaldehyde and labeled with filipin as described in Materials and Methods. Arrows indicate specific regions of perinuclear DHE labeling that colocalize with FITC-anti-Tac antibody. Bar = 10 μm.

after photobleaching, and panels *c* and *f* 20 min after recovery from photobleaching. Panels *a–c* show a cell where the fluorescence of a section of the plasma membrane was bleached (*arrows*). As seen in panel *c*, after 20 min at 37°C, a significant fraction of the fluorescence in the bleached area had recovered. There also appears to be a concomitant

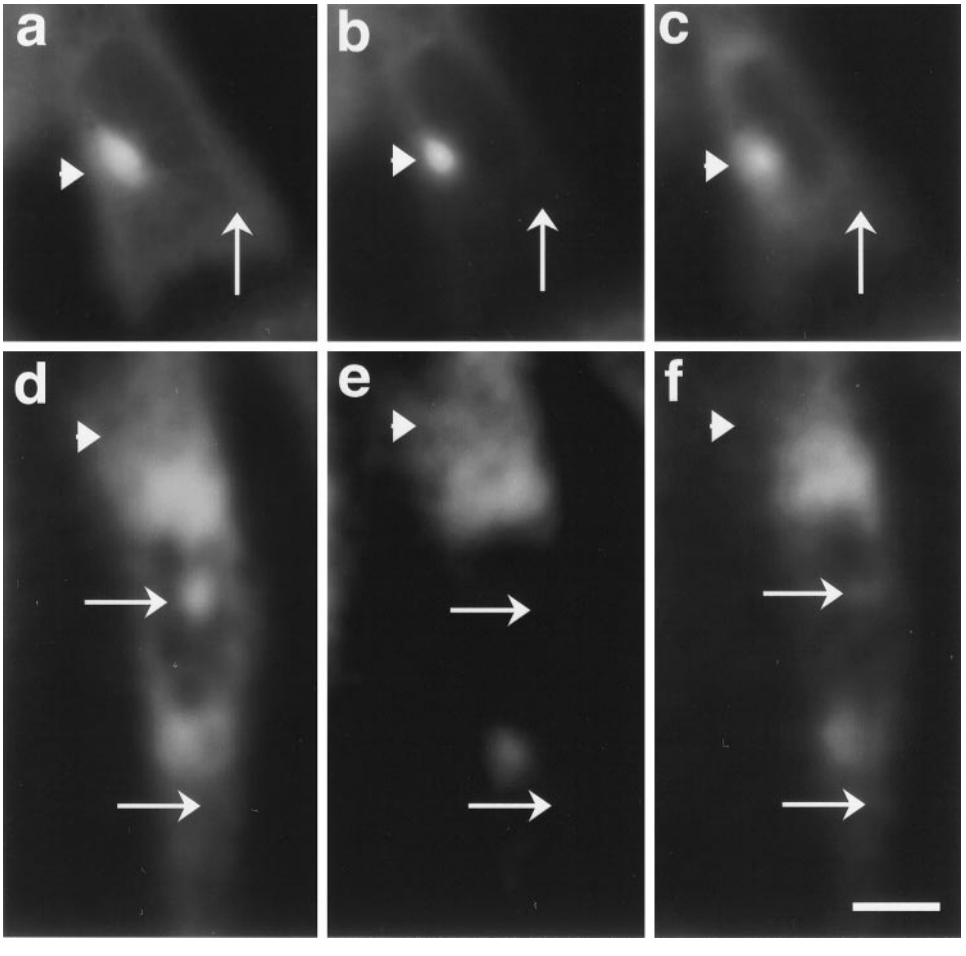

FIGURE 7 TRVb-1/TacTGN38 cells labeled with 12.5 μM DHE. Two different fields of cells were imaged for DHE fluorescence (*a* and *d*). The field iris was then closed and the small area now illuminated was bleached by keeping the excitation shutter open for 1 min. Images of these cells taken immediately after bleaching and reopening the field iris are shown in (*b*) and (*e*). The dishes were then kept on the microscope stage at 37°C for 20 min, following which the cells were imaged again (*c* and *f*). The areas where photobleached fluorescence recovered are shown with arrows. Dimming of membrane areas that presumably donated DHE resulting in the recovery are shown with arrowheads. Bar = 10 μm.

decrease in the intensity of the intracellular fluorescent compartment (*arrowheads*). These observations are also borne out by quantitative analyses shown in Fig. 8. The quantitative analysis was carried out using the protocol discussed in Materials and Methods. From this figure (panels *a–c*), we find that the intracellular pool is about three times brighter than the average plasma membrane fluorescence for this cell. The first set of three columns shows the fluorescence intensity ratio in the intracellular fluorescent compartment to that on the unbleached part of the plasma membrane. Immediately after bleaching, we find a decrease in this ratio, suggesting that a part of the intracellular fluorescence was also bleached in the bleaching process. After 20 min, this ratio recovers to a substantial extent. This could mean that some of the bleached fluorescence in the intracellular pool recovered as a result of delivery of DHE from the plasma membrane, and/or that the fluorescence intensity in the denominator, i.e., in the unbleached part of the plasma membrane, decreased because of the delivery of some of the fluorescence from this part of the membrane to other bleached regions. Similarly, in the second set of three columns, we see that the ratio of fluorescence intensity in the bleached part of the plasma membrane to that in the unbleached part decreased significantly after bleaching, and recovered almost completely within 20 min. Panels *d–f* show a second example in which the intracellular DHE pool and part of the plasma membrane fluorescence from the region around it are bleached. Twenty minutes after the bleaching, a fraction of the intracellular fluorescence is seen to recover (*arrow*) in addition to most of the plasma membrane fluorescence in the bleached region (also shown by arrow). A fraction of fluorescence in the unbleached region of the plasma membrane is lost during this time (*arrowhead*). These results are also confirmed quantitatively in Fig. 8. These experiments indicate that it is possible to follow trafficking of DHE among various cellular locations in living cells, and opens up the possibility of addressing specific questions regarding the mechanism and kinetics of these processes.

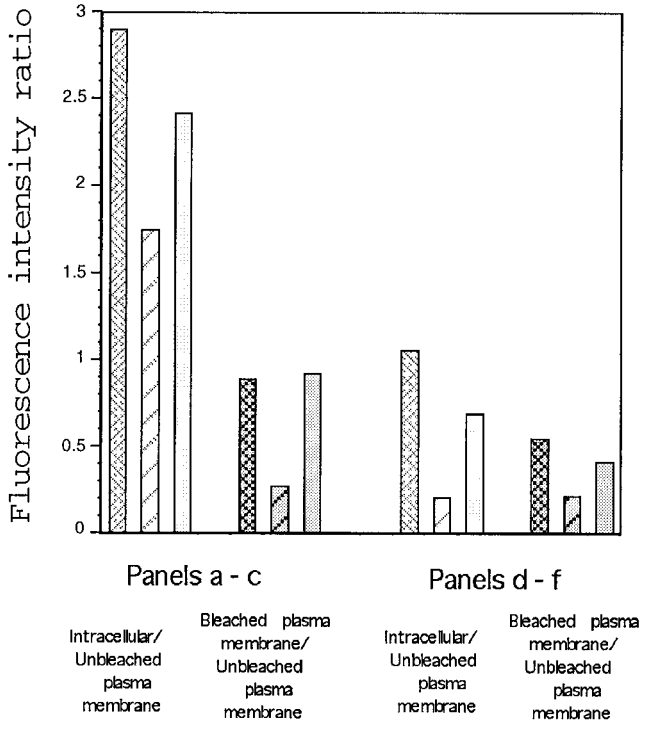

FIGURE 8 Quantification of fluorescence photobleaching recovery experiments shown in Fig. 7. The first two sets of three columns each correspond to panels *a–c* in Fig. 7 and the last two sets correspond to panels *d–f*. The first and third sets of columns represent the ratios of fluorescence intensities in the intracellular fluorescent compartment to that in the unbleached part of the plasma membrane. The second and fourth sets represent the intensity ratios of the bleached to the unbleached parts of the plasma membrane. Within each set of three columns, the first (*cross-hatched*) column represents the ratio before photobleaching, the second (*hatched*) column represents the ratio immediately after photobleaching, and the third (*shaded*) column represents the ratio 20 min after recovery at 37°C.

DISCUSSION

Fluorescence imaging of DHE, which absorbs and emits in the UV region of the spectrum, was made possible by the use of a camera with a back-thinned CCD chip having high quantum efficiency at these wavelengths. Direct observation of DHE fluorescence in living cells and the observation of filipin bound to cholesterol in fixed cells provide two independent probes of cholesterol distribution. With both these methods, the ERC and the TGN were seen to be the major sites of intracellular cholesterol in CHO cells. Although the intracellular distributions of both cholesterol tracers were similar, the labeling of the plasma membrane by DHE was not as prominent as the filipin staining for most cells. There could be several explanations for this difference. First, it should be noted that labeling cells with filipin requires fixation followed by long incubations at room temperature. Because cholesterol itself cannot be fixed by these fixation methods and cholesterol interbilayer exchange is rapid on the time scale of the experimental manipulations (Yeagle, 1985; Schroeder et al., 1995), it is not possible to rule out a redistribution of cholesterol due to binding and sequestration of a fraction of cholesterol by filipin. In fact, filipin has been shown to extract cholesterol from the host membranes (Beknke et al., 1984). Furthermore, as seen from the images presented in this paper, the long paraformaldehyde fixation required for filipin labeling itself compromises the morphology of the plasma membrane, and may reorganize membrane components. It is also possible that some intracellular membranes are not as accessible to filipin as the plasma membrane, even after prolonged incubations. For example, it was initially suggested from filipin binding studies that the clathrin-coated pits are lower in cholesterol than the surrounding plasma membrane (Montesano et al., 1979, 1981). However, when coated vesicles were isolated and the coats removed, there was an enhanced binding of filipin to these membranes, suggesting

that the coats were somehow restricting the access of filipin to the coated pits (Steer et al., 1984). False-negative cytochemical results using filipin as a tracer for cellular cholesterol has also been reported by other authors (Pelletier and Vitale, 1994).

Alternatively, although DHE has been shown in several instances to mimic cholesterol distribution (Fischer et al., 1984; Schroeder et al., 1987, 1991, 1995), the three additional double bonds and the extra methyl group could result in alterations in the conformation of the molecule relative to cholesterol (e.g., an alteration in ring puckering and a partial loss of the flexibility of the seven-membered alkyl chain). These alterations could, in turn, result in somewhat different interactions of this derivative with the bilayer compared to native cholesterol. In fact, subtle differences in the lateral distribution of cholesterol, ergosterol, and DHE in model membranes at steady state has been previously reported (Liu et al., 1997). Furthermore, it is not clear whether DHE can be esterified and metabolized in mammalian cells as efficiently as native cholesterol. Inadequate metabolic turnover of DHE in these cells may affect the overall cholesterol homeostatic mechanisms, resulting in its altered steady-state distribution. Despite these potential complications, however, it is encouraging to note that both DHE and filipin show similar ERC/TGN distributions in these cells.

Implications of the ERC/TGN cholesterol pool in cellular cholesterol homeostasis

Results presented here in Figs. 5 and 6 show that a very large fraction of the intracellular cholesterol pool is localized in the ERC and the TGN. This observation is very interesting, since it corroborates and extends several previous findings. For example, it is known that cells regulate their total cholesterol content as well as inter-organellar distribution rather stringently (Brown and Goldstein, 1986; Liscum and Dahl, 1992). This homeostasis appears to operate primarily by a balance between cholesterol biosynthesis, which is determined by the turnover of the rate-limiting enzyme HMG-CoA reductase in a cholesterol-responsive manner, and the esterification and storage of excess cholesterol by the enzyme ACAT (Brown and Goldstein, 1986; Liscum and Dahl, 1992). However, ACAT is predominantly localized at the ER membrane that contains a very small fraction of total cellular cholesterol. In addition, ACAT has been previously shown to be activated by an increase in the total cholesterol pool at the plasma membrane, and not directly by the cholesterol released in the lysosomes from internalized lipoproteins (Xu and Tabas, 1991). One question that has remained unanswered is how the ER-resident ACAT senses cholesterol buildup at the plasma membrane. Since both the TGN and the ERC are intracellular sites that continually exchange membrane with the plasma membrane (Mukherjee et al., 1997), these sites appear to be ideal targets for triggering ACAT activation in response to cholesterol buildup at the plasma membrane. Indeed, the Golgi apparatus and the TGN have been previously implicated as organelles playing an important role in cellular cholesterol homeostasis (Coxey et al., 1993; Hasumi et al., 1993; Mendez, 1995). In addition, a recent report suggests that recycling endosomes isolated from rat livers may be involved in the cell surface delivery of lipoprotein-derived cholesterol (Hornick et al., 1997). It is possible that direct cholesterol delivery occurs from the ERC and/or TGN membrane to the ramified ER in the pericentriolar region where both ERC and TGN reside in CHO cells. Such cholesterol delivery may occur by direct access of the ER-resident ACAT active site to cholesterol in the ERC or the TGN membrane (due to spatial proximity), or it might involve desorption and delivery of cholesterol to ACAT either by passive diffusion or aided by sterol-binding proteins. Recently, it has been shown by immunofluorescence that there is a non-ER pool of ACAT that concentrates in the juxtanuclear region of macrophages (Khelef et al., 1998). Studies are in progress to determine whether this concentration of ACAT near the nucleus is in the ERC or the TGN. In addition, it should be noted that some recent studies suggest that a fraction of lipoprotein-derived cholesterol may be directly esterified by ACAT without going through the plasma membrane (Neufeld et al., 1996; Underwood et al., 1998). The pool of ACAT that catalyzes such esterification has not been characterized.

Implication of ERC/TGN cholesterol localization in intracellular trafficking of lipid analogs and lipid-anchored proteins

In addition to the maintenance of cellular cholesterol homeostasis, the large intracellular cholesterol pool localized at the ERC of CHO cells might explain some other recent observations regarding the trafficking of lipids and lipid-anchored proteins in these cells. We have recently shown that lipid analogs with identical headgroup chemistry and varying solely in the composition of their hydrophobic tails (chain length or unsaturation), traffic to different intracellular locations in CHO cells after being endocytosed. We have also shown that this differential trafficking of the lipid analogs can be explained by their preference to partition into membrane domains of varying motional characteristics and/or curvatures (S. Mukherjee, T. T. Soe, and F. R. M. Maxfield, submitted for publication) and can be modulated by altering cellular cholesterol contents (S. Mukherjee and F. R. Maxfield, unpublished observations). It is known from extensive studies in model membrane systems that the precise amount of cholesterol in a membrane bilayer strongly affects the formation and the properties of lateral membrane domains (Almeida et al., 1993; Silvius et al., 1996). Thus, by placing a significant fraction of cellular cholesterol in the ERC, our results rationalize the presence of lateral membrane domains of varying properties in the organelles along the endocytic pathway.

Similarly, data from our laboratory have shown that although GPI-anchored proteins are internalized into cells at

approximately similar rates as other membrane markers such as short chain fluorescent sphingomyelin analogs, they are retained ~3 times longer in the ERC before they are recycled (Mayor, et al., 1998). Interestingly, this enhanced retention can be countered if cells are grown under conditions where their intracellular cholesterol pool is depleted by ~40%. This observation strongly suggests a role for cholesterol in the retention of the GPI-anchored proteins in the ERC. The observation that the ERC is indeed an organelle that is enriched in cholesterol is supportive of this organelle playing a role in the selective retention of certain molecules, thereby affecting their overall kinetics of trafficking.

In conclusion, we show that cholesterol distribution and trafficking can be followed in living cells by using cholesterol analogs such as DHE. Such analogs offer an extremely powerful tool to address unresolved questions regarding the role of cholesterol in the structural modulation of bilayer properties, as well as its functional implications.

We thank Dr. A. Chattopadhyay (Centre for Cellular and Molecular Biology, Hyderabad, India) for the kind gift of 25-NBD-cholesterol, Dr. W. G. Mallet (Cornell University Medical College, NY) for the FITC labeled anti-Tac antibody, and Paul Mellman of Chroma Technology for assistance with the UV filters. S.M. acknowledges a postdoctoral fellowship from the Norman and Rosita Winston Foundation for Biomedical Research.

This work was supported by Grant DK27083 from the National Institutes of Health and by a grant from the Human Frontiers Science Program.

REFERENCES

Ahmed, S. N., D. A. Brown, and E. London. 1997. On the origin of sphingolipid/cholesterol-rich detergent-insoluble cell membranes: physiological concentrations of cholesterol and sphingolipid induce formation of a detergent-insoluble, liquid-ordered lipid phase in model membranes. *Biochemistry*. 36:10944–10953.

Almeida, P. F. F., W. L. C. Vaz, and T. E. Thompson. 1993. Percolation and diffusion in three-component lipid bilayers: effect of cholesterol on an equimolar mixture of two phosphatidylcholines. *Biophys. J.* 64: 399–412.

Beknke, O., J. Tranum-Jensen, and B. van Deurs. 1984. Filipin as a cholesterol probe. I. Morphology of filipin-cholesterol interaction in lipid model systems. *Eur. J. Cell Biol.* 35:189–199.

Brown, M. S., and J. L. Goldstein. 1986. A receptor-mediated pathway for cholesterol homeostasis. *Science*. 232:34–47.

Coxey, R. A., P. G. Pentchev, G. Campbell, and E. J. Blanchette-Mackie. 1993. Differential accumulation of cholesterol in Golgi compartments of normal and Niemann-Pick type C fibroblasts incubated with LDL: a cytochemical freeze-fracture study. *J. Lipid Res.* 34:1165–1176.

Duax, W. L., Z. Wawrzak, J. F. Griffin, and C. Cheer. 1988. Sterol conformation and molecular properties. *In* Biology of Cholesterol. P. L. Yeagle, editor. CRC Press, Boca Raton, Florida. 1–18.

Dunn, K., and F. R. Maxfield. 1998. Ratio imaging instrumentation. *Methods Cell Biol.* 56:217–236.

Fischer, R. T., F. A. Stephenson, A. Shafiee, and F. Schroeder. 1984. Delta 5,7,9(11)-Cholestatrien-3-β-ol: a fluorescent cholesterol analogue. *Chemis. Phys. Lipids*. 36:1–14.

Harris, J. S., D. E. Epps, S. R. Davio, and F. J. Kezdy. 1995. Evidence for transbilayer, tail-to-tail cholesterol dimers in dipalmitoylglycerophosphocholine liposomes. *Biochemistry*. 34:3851–3857.

Hasumi, K., S. Naganuma, J. Koshizawa, H. Mogi, and A. Endo. 1993. Stimulation of acyl-CoA:cholesterol acyltransferase activity by brefeldin A in macrophage J774 cells. *Biochim. Biophys. Acta*. 1167:155–158.

Hornick, C. A., D. Y. Hui, and J. G. De Lamatre. 1997. A role for retrosomes in intracellular cholesterol transport from endosomes to the plasma membrane. *Am. J. Physiol.* 273:C1075–C1081.

Humphrey, J. S., P. J. Peters, L. C. Yuan, and J. S. Bonifacino. 1993. Localization of TGN38 to the trans-Golgi network: involvement of a cytoplasmic tyrosine-containing sequence. *J. Cell Biol.* 120:1123–1135.

Johnson, A. O., R. N. Ghosh, K. W. Dunn, R. Garippa, G. Park, S. Mayor, F. R. Maxfield, and T. E. McGraw. 1996. Transferrin receptor containing the SDYQRL motif of TGN38 causes a reorganization of the recycling compartment but is not targeted to the TGN. *J. Cell Biol.* 135:1749–1762.

Khelef, N., X. Buton, N. Beatini, H. Wang, V. Meiner, T.-Y. Chang, R. V. Farese, Jr., F. R. Maxfield, and I. Tabas. 1998. Immunolocalization of ACAT in macrophages. *J. Biol. Chem.* 273:11218–11224.

Koval, M., and R. E. Pagano. 1989. Lipid recycling between the plasma membrane and intracellular compartments: transport and metabolism of fluorescent sphingomyelin analogues in cultured fibroblasts. *J. Cell Biol.* 108:2169–2181.

Lange, Y. 1991. Disposition of intracellular cholesterol in human fibroblasts. *J. Lipid Res.* 32:329–339.

Liscum, L., and N. K. Dahl. 1992. Intracellular cholesterol transport. *J. Lipid Res.* 33:1239–1254.

Liscum, L., and K. W. Underwood. 1995. Intracellular cholesterol transport and compartmentation. *J. Biol. Chem.* 270:15443–15446.

Liu, F., I. P. Sugar, and P. L. Chong. 1997. Cholesterol and ergosterol superlattices in three-component liquid crystalline lipid bilayers as revealed by dehydroergosterol fluorescence. *Biophys. J.* 72:2243–2254.

Mayor, S., J. F. Presley, and F. R. Maxfield. 1993. Sorting of membrane components from endosomes and subsequent recycling to the cell surface occurs by a bulk flow process. *J. Cell Biol.* 121:1257–1269.

Mayor, S., S. Sabharanjak, and F. R. Maxfield. 1998. Cholesterol-dependent retention of GPI-anchored proteins in endosomes. *EMBO J.* 17:4626–4638.

Mendez, A. J. 1995. Monensin and brefeldin A inhibit high density lipoprotein-mediated cholesterol efflux from cholesterol-enriched cells. Implications for intracellular cholesterol transport. *J. Biol. Chem.* 270: 5891–5900.

Montesano, R., A. Perrelet, P. Vassalli, and L. Orci. 1979. Absence of filipin-sterol complexes from large coated pits on the surface of culture cells. *Proc. Natl. Acad. Sci. U.S.A.* 76:6391–6395.

Montesano, R., P. Vassalli, and L. Orci. 1981. Structural heterogeneity of endocytic membranes in macrophages as revealed by the cholesterol probe, filipin. *J. Cell Sci.* 51:95–107.

Moore, E. D. W., P. L. Becker, K. E. Fogarty, D. A. Williams, and F. S. Fay. 1990. Ca^{2+} imaging in single living cells: theoretical and practical issues. *Cell Calcium*. 11:157–179.

Mukherjee, S., and A. Chattopadhyay. 1996. Membrane organization at low cholesterol concentrations: a study using 7-nitrobenz-2-oxa-1,3-diazol-4-yl-labeled cholesterol. *Biochemistry*. 35:1311–1322.

Mukherjee, S., R. N. Ghosh, and F. R. Maxfield. 1997. Endocytosis. *Physiol. Rev.* 77:759–803.

Neufeld, E. B., A. M. Cooney, J. Pitha, E. A. Dawidowicz, N. K. Dwyer, P. G. Pentchev, and E. J. Blanchette-Mackie. 1996. Intracellular trafficking of cholesterol monitored with a cyclodextrin. *J. Biol. Chem.* 271:21604–21613.

Pelletier, R. M., and M. L. Vitale. 1994. Filipin vs. enzymatic localization of cholesterol in guinea pig, mink, and mallard duck testicular cells. *J. Histochem. Cytochem.* 42:1539–1554.

Salzman, N. H., and F. R. Maxfield. 1989. Fusion accessibility of endocytic compartments along the recycling and lysosomal endocytic pathways in intact cells. *J. Cell Biol.* 109:2097–2104.

Schroeder, F., Y. Barenholz, E. Gratton, and T. E. Thompson. 1987. A fluorescence study of dehydroergosterol in phosphatidylcholine bilayer vesicles. *Biochemistry*. 26:2441–2448.

Schroeder, F., J. R. Jefferson, A. B. Kier, J. Knittel, T. J. Scallen, W. G. Wood, and I. Hapala. 1991. Membrane cholesterol dynamics: cholesterol domains and kinetic pools. *Proc. Soc. Exp. Biol. Med.* 196: 235–252.

Schroeder, F., J. K. Woodford, J. Kavecansky, W. G. Woods, and C. Joiner. 1995. Cholesterol domains in biological membranes. *Mol. Membr. Biol.* 12:113–119.

Severs, N. J. 1982. Cholesterol distribution and structural differentiation in the sarcoplasmic reticulum of rat cardiac muscle cells. A freeze-fracture cytochemical investigation. *Cell Tissue Res.* 224:613–624.

Silvius, J. R., D. del Giudice, and M. Lafleur. 1996. Cholesterol at different bilayer concentrations can promote or antagonize lateral segregation of phospholipids of differing acyl chain length. *Biochemistry*. 35: 15198–15208.

Simons, K., and E. Ikonen. 1997. Functional rafts in cell membranes. *Nature*. 387:569–572.

Slotte, J. P. 1995. Lateral domain formation in mixed monolayers containing cholesterol and dipalmitoylphosphatidylcholine or N-palmitoylsphingomyelin. *Biochim. Biophys. Acta*. 1235:419–427.

Slotte, J. P., and P. Mattjus. 1995. Visualization of lateral phases in cholesterol and phosphatidylcholine monolayers at the air/water interface—a comparative study with two different reporter molecules. *Biochim. Biophys. Acta* 1254:22–29.

Steer, C. J., M. Bisher, R. Blumenthal, and A. C. Steven. 1984. Detection of membrane cholesterol by filipin in isolated rat liver coated vesicles is dependent upon removal of the clathrin coat. *J. Cell Biol.* 99:315–319.

Tabas, I. 1997. Free cholesterol-induced cytotoxicity. A possible contributing factor to macrophage foam cell necrosis in advanced atherosclerotic lesions. *Trends Cardiovasc. Med.* 7:256–263.

Tabas, I., X. Zha, N. Beatini, J. N. Myers, and F. R. Maxfield. 1994. The actin cytoskeleton is important for the stimulation of cholesterol esterification by atherogenic lipoproteins in macrophages. *J. Biol. Chem.* 269:22547–22556.

Underwood, K. W., N. L. Jacobs, A. Howley, and L. Liscum. 1998. Evidence for a cholesterol transport pathway from lysosomes to the endoplasmic reticulum that is independent of the plasma membrane. *J. Biol. Chem.* 273:4266–4274.

Vaz, W. L. C., and P. F. F. Almeida. 1993. Phase topology and percolation in multi-lipid bilayers: is the biological membrane a domain mosaic? *Curr. Opin. Struct. Biol.* 3:482–488.

Xu, X. X., and I. Tabas. 1991. Lipoproteins activate acyl-coenzyme A:cholesterol acyltransferase in macrophages only after cellular cholesterol pools are expanded to a critical threshold level. *J. Biol. Chem.* 266:17040–17048.

Yamashiro, D. J., B. Tycko, S. R. Fluss, and F. R. Maxfield. 1984. Segregation of transferrin to a mildly acidic (pH 6.5) para-Golgi compartment in the recycling pathway. *Cell*. 37:789–800.

Yeagle, P. L. 1985. Cholesterol and the cell membrane. *Biochim. Biophys. Acta* 822:267–287.